Int. J. Solids Structures Vol. 22, No. 7, pp. 709–719, 1986
Printed in Great Britain.

0020-7683/86 $3.00+.00
Pergamon Journals Ltd.

NUMERICAL INVESTIGATIONS OF CRACK CLOSURE INTEGRAL AND J-INTEGRAL CALCULATIONS FOR A THERMALLY STRESSED SPECIMEN

F.-G. BUCHHOLZ
Universität—Gesamthochschule—Paderborn, Fachbereich 10, D-4790 Paderborn, Federal Republic of Germany

and

H. GREBNER and U. STRATHMEIER
Brown, Boveri & Cie AG, D-6800 Mannheim, Federal Republic of Germany

(*Received* 25 *April* 1985)

Abstract—Among the various numerical procedures used in fracture analysis the modified crack closure integral method given by Rybicki and Kanninen is a numerically very effective procedure in combination with constant strain elements. Based on an analytical energy consideration for a thermally stressed specimen under plain strain conditions it will be shown, that the method can be extended for the application with higher order finite elements, keeping its original advantages. By comparing results calculated with a global energy and the *J*-integral method it will be shown, that the improved modified crack closure integral method computes the energy release rate with extending crack length with very good efficiency and accuracy.

1. INTRODUCTION

Among the various numerical procedures used in fracture analysis, such as extrapolation methods[1], superposition methods[2] and energy methods[3–7] the modified crack closure integral method given by Rybicki and Kanninen[8] is a very straightforward and effective numerical procedure. This procedure delivers simultaneously the separated energy release rated $G_i(a)$, i = I, II, III for mixed-mode crack tip conditions from just one finite element analysis per crack length a.

Using "Constant Strain Elements" (CSE) the method has been applied in Ref. [8] to different fracture problems involving coplanar crack extension and in all cases the numerical results were in good agreement with reference solutions. But different from general experience with higher order finite elements[10] Rybicki and Kanninen have reported in Ref. [8] on a considerable decrease of accuracy when their method has been used in combination with higher order elements. To investigate this irregular effect in detail, the specially supported specimen of Fig. 1 will be considered, for which we can deduce a very useful analytical reference value for the overall strain energy of the uncracked specimen generated by a homogeneous temperature decrease of the strip.

2. GLOBAL ENERGY METHODS

2.1. *The uncracked specimen*

If the uncracked strip of finite width illustrated in Fig. 1 is subjected to a homogeneous temperature decrease $\Delta T = \text{const} < 0$ it can be shown that the generated elastic strain energy $U = U^{y,z}$ $(a = 0)$ can be separated into two uncoupled terms U^z $(a = 0)$ due to the suppressed displacements in the z-direction (causing plane strain conditions) and U^y $(a = 0)$ due to the suppressed displacements in the y-direction. Starting from the constitutive equations of linear thermoelasticity[9] with $\Delta T = \text{const} < 0$ and $\varepsilon_{zz} = \varepsilon_{yy} = 0$ according to the suppressed displacements in the y- and z-directions and $\sigma_{xx} = 0$ due to the unrestricted displacements in the x-direction one can find for the uncracked thermally stressed tension

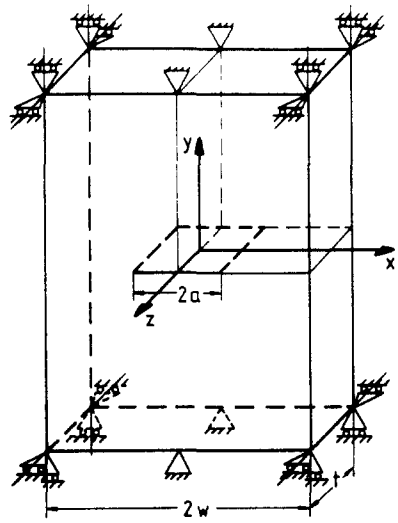

Fig. 1. Thermally stressed specimen ($\Delta T = -100°C$; material: Al; dimensions: $w = 15$ mm, $h = 13$ mm, $t = 1$ mm).

strip of Fig. 1 (with E Young's modulus, ν Poisson's ratio, α linear coefficient of thermal expansion)

$$\varepsilon_{xx} = \frac{1+\nu}{1-\nu}\alpha\Delta T, \tag{1}$$

$$\sigma_{yy} = -\frac{E\alpha\Delta T}{1-\nu} \tag{2}$$

and

$$\sigma_{zz} = -\frac{E\alpha\Delta T}{1-\nu}. \tag{3}$$

Substituting these results into the general 3D-formula for the elastic strain energy:

$$U(a=0) = \int_V \tfrac{1}{2}\sigma_{ij}(\varepsilon_{ij} - \alpha\Delta T\delta_{ij})\,\mathrm{d}V, \tag{4}$$

one gets

$$U(a=0) = \frac{E}{1-\nu}(\alpha\Delta T)^2 V = U^{y,z}(a=0), \tag{5}$$

due to the temperature change ΔT and the suppressed displacements in the y- and z-directions. Using the 2D-form of eqn (4) for plane strain conditions one finds

$$U_{\text{pl.strain}}(a=0) = \frac{1}{2}\frac{1+\nu}{1-\nu}E(\alpha\Delta T)^2 V = U^{y}(a=0), \tag{6}$$

due to the suppressed displacements in the y-direction alone and

$$U^{z}(a=0) = U^{y,z}(a=0) - U^{y}(a=0), \tag{7}$$

resulting in

$$U^z(a = 0) = \tfrac{1}{2}E(\alpha\Delta T)^2 V. \tag{8}$$

On the other hand for both separated parts of the completely cracked specimen ($a = w$) it holds according to eqn (4).

$$U(a = w) = 2\left[\tfrac{1}{2}E(\alpha\Delta T)^2\frac{V}{2}\right] = U^z(a = w) \tag{9}$$

and with reference to eqn (6)

$$U_{\text{pl.strain}}(a = w) = 0 = U^y(a = w). \tag{10}$$

From comparing eqns (8) and (9) it finally can be concluded that only the separated and uncoupled part U^y ($a = 0$) of the elastic strain energy generated by the homogeneous temperature decrease ΔT can be released from the specimen to the crack. Consequently, with U^y ($a = 0$) an analytical reference value is given, for that part of the elastic strain energy that may initiate and propagate the crack until complete separation of the specimen.

2.2. *The cracked specimen*

For the cracked specimen of Fig. 1 no analytical solution of the corresponding mixed boundary value problem is available. But it has been shown in Ref. [13] that on the basis of the following relations

$$\tilde{U}^y(a) = \tfrac{1}{2}\mathbf{r}_e^T(a)\mathbf{K}(a)\mathbf{r}_e(a) \tag{11}$$

and

$$G(a) = -\lim_{\Delta a \to 0}\frac{\tilde{U}^y(a+\Delta a) - \tilde{U}^y(a)}{t\Delta a} = -\frac{\mathrm{d}\tilde{U}^y(a)}{t\,\mathrm{d}a}, \tag{12}$$

the global energy release rate $G(a)$ with extending crack length a can be computed with very good accuracy, if sophisticated procedures are used for the required numerical differentiation $\mathrm{d}\tilde{U}^y/\mathrm{d}a$ (global energy method—EN). In eqn (11) $\mathbf{r}_e(a) = \mathbf{r}_a(a) - \mathbf{r}_0(a = 0)$ denotes the global vector of the effective nodal point displacements ($\mathbf{r}_a(a)$ actual displacements, $\mathbf{r}_0(a = 0)$ unrestricted displacements due to $\Delta T = \text{const}$, $\mathbf{r}^T$ transposed vector) and $\mathbf{K}(a)$ is the global stiffness matrix.

In Fig. 3 the decrease of the elastic strain energy $\tilde{U}^y(a)$ of the thermally stressed specimen ($\Delta T = -100°\text{C}$) is plotted vs crack length, as calculated for the two different LSE-net topologies of Figs. 2(a) and (b).

It can be seen that for the fine net, F, and the superfine net, S, the plots nearly coincide and that for $a = w$ the specimen still contains a small amount of strain energy $\tilde{U}_R(a = w)$ as long as the last pair of nodal points is still connected. In Fig. 4 the corresponding energy release rates $G(a)$, [here identical to $G_I(a)$] calculated from eqn (12) are plotted vs crack length ratio a/w. For the net, F and S one also gets nearly coinciding graphs (G1–EN–F and S) showing increasing $G_I(a)$—values up to $a/w \approx 0.5$ and a nearly stationary value for $0.5 \lesssim a/w \lesssim 0.9$. Interesting is the result, that with the superfine net, S, $G_I(a)$ keeps the stationary value till higher ratios a/w during crack extension towards the free surface.

On the basis of the following relations

$$U^y_{\text{ref}}(a = 0) \overset{\nabla}{\underset{\circ}{=}} \hat{U}^y(a = w) = 2t\int_{a=0}^{a=w} G(a)\,\mathrm{d}a \tag{13}$$

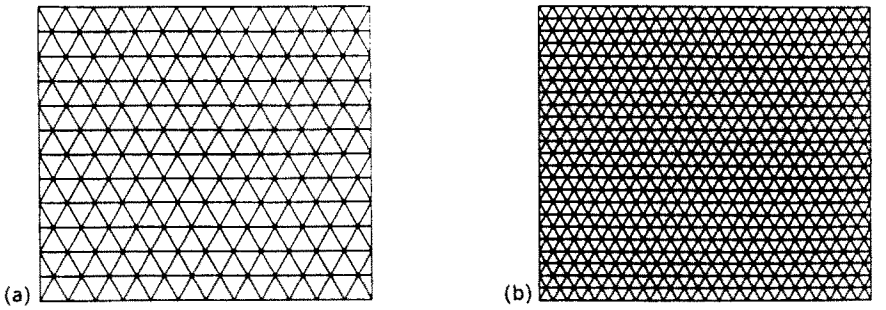

Fig. 2. Finite element nets of the specimen (one quarter) used for the ASKA calculations of $G(a)$. Triangular 6-node "Linear Strain Elements" (LSE): (a) fine net, F, 300 elements, 649 nodal points; (b) superfine net, S, 1176 elements, 2449 nodal points.

and

$$U^{v}_{\mathrm{ref}}(a=0) = U^{v}(a=0) - \tilde{U}^{v}_{R}(a=w), \tag{14}$$

a quantitative measure of accuracy can be established for the numerical methods used to calculate the energy release rates with extending crack length[11–13]. Equation (13) states that the elastic strain energy $\hat{U}^{v}(a=w)$ which the specimen releases to the crack until complete separation ($a=w$) must be equal to the separated energy term $U^{v}(a=0)$ of the uncracked specimen reduced by the rest energy $\tilde{U}_{R}(a=w)$. Referring to eqn (13) we now can compute by

$$\Delta_{\mathrm{rel}} = \frac{\hat{U}^{v}(a=w) - U^{v}_{\mathrm{ref}}(a=0)}{U^{v}_{\mathrm{ref}}(a=0)}, \tag{15}$$

the relative overall difference of these values. For the fine net, F, this results in $\Delta_{\mathrm{rel}} = -1.4\%$ and for the superfine net, S, one gets $\Delta_{\mathrm{rel}} = -0.02\%$ which indeed confirms this plot as a reference curve for the following investigations of some local energy methods for the calculation of $G(a)$ with increasing crack length.

3. LOCAL ENERGY METHODS

3.1. *Crack closure integral and modified crack closure integral calculations*

Referring to Fig. 5 and its notations one can write according to Irwin[14] the following

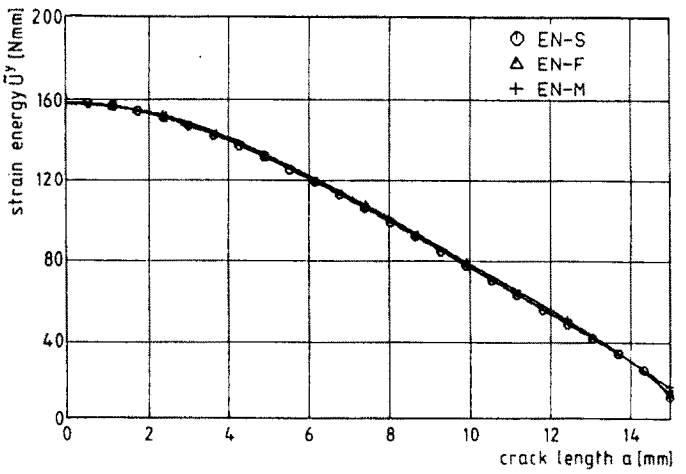

Fig. 3. Elastic strain energy of the cracked specimen vs crack length calculated with the global energy method, EN.

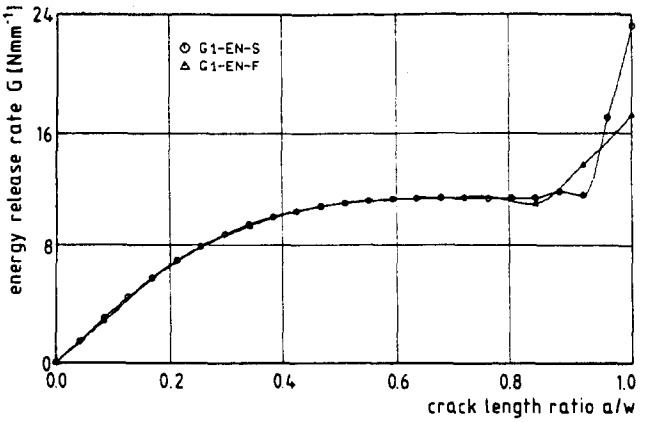

Fig. 4. Energy release rate of the cracked specimen vs crack length ratio calculated with the global energy method, EN.

well-known crack closure integral relation

$$-\frac{\mathrm{d}U^{\gamma}(a)}{t\,\mathrm{d}a} = G_{\mathrm{I}}(a) = \lim_{\delta a \to 0} \frac{2}{\delta a} \int_{x=0}^{x=\delta a} \frac{1}{2} \sigma_{yy}(r = x, \varphi = 0) u_y(r = \delta a - x, \varphi = \pi)\,\mathrm{d}x \tag{16}$$

for the specimen of Fig. 1 under consideration of its special supports and its thermal loading. The physical meaning of eqn (16) is, that for elastic systems the change of the strain energy due to crack extension by δa and the work required to close the crack by δa to its original length have to be of equal values.

Following Ref. [8], eqn (16) can be transformed into an appropriate finite element representation given by

$$G_{\mathrm{I}}(a) = \frac{1}{t} \lim_{\Delta a \to 0} \frac{1}{\Delta a} \frac{1}{2} F_{y,i-1}(a) \Delta u_{y,i-1}(a), \tag{17}$$

where the CSE-net of Fig. 6(a) has been incorporated. To avoid an extra finite element analysis for the calculation of the unknown nodal point force $F_{y,i-1}$ in eqn (17), Rybicki and Kanninen[8] started from the basic assumption, that for $\Delta a \to 0$ the crack tip nodal point force $F_{y,i}$ should be a good approximation for the actually required force $F_{y,i-1}$. This leads to the following equation

$$G_{\mathrm{I}}(a) = \frac{1}{t} \lim_{\Delta a \to 0} \frac{1}{\Delta a} \frac{1}{2} F_{y,i}(a) \Delta u_{y,i-1}(a), \tag{18}$$

here referred to as the CSE-Formula of 1st-Order. The results given in Ref. [8] justified the

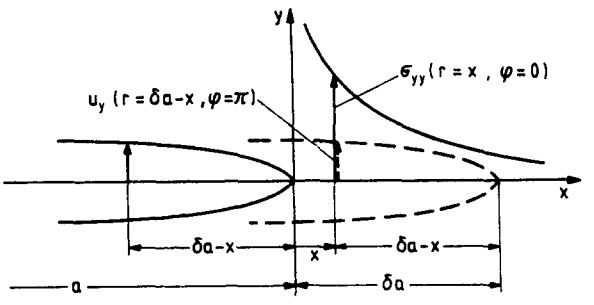

Fig. 5. Irwin's crack closure integral.

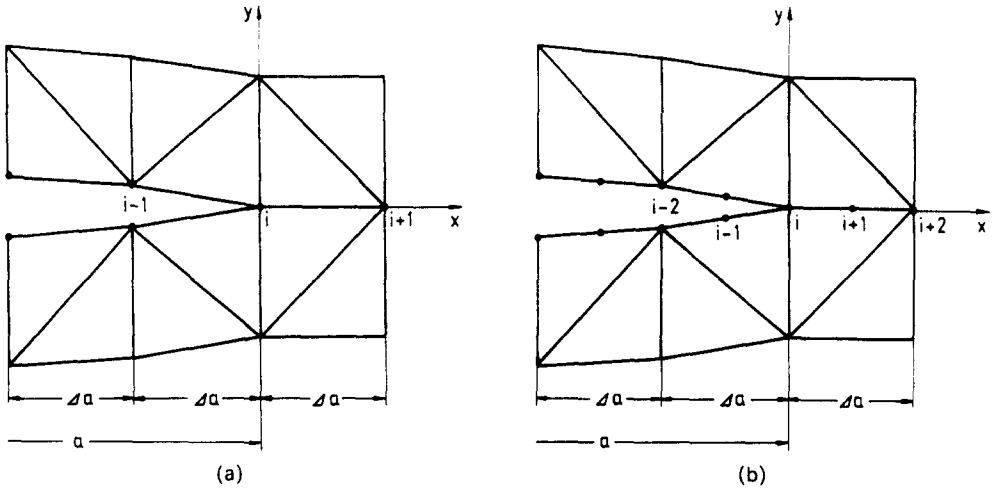

Fig. 6. Finite element nets around the crack tip: (a) CSE-net; (b) LSE-net.

basic assumption and proved the modified crack closure integral method to be a very straightforward and effective numerical procedure for calculating energy release rates with crack extension in combination with CSE-nets.

In order to utilize the well-known advantages of higher order finite elements, for example of the "Linear Strain Elements" (LSE) of Fig. 6(b), eqn (18) can be adapted to this case in the following straightforward way

$$G_I(a) = \frac{1}{t} \lim_{\Delta a/2 \to 0} \frac{1}{\Delta a} F_{y,i}(a) \Delta u_{y,i-1}(a). \tag{19}$$

According to Rybicki and Kanninen's basic assumption it has to be considered that in this LSE-Formula of 1st-Order the crack will only be closed by the amount $\Delta a/2$. It has been shown by Refs [11, 12] that eqn (19) can be applied in fracture analysis with some advantages compared to eqn (18) if crack tip positions $i-1$ at midside nodes of the LS-Elements (Fig. 6(b)) are avoided, which create interelement incompatibilities in front of the crack tip. But the detailed analysis by the aid of the global energy method—EN [eqns (11, 12)] and the analytical accuracy measure [eqns (13–15)] in form of the results in Figs 7 and 8 will show, that eqn (18) still has to be improved for the use in combination with LS-Elements[13].

Starting with Fig. 7, the G1–RK–F plot, calculated with eqn (19) and the LSE-net, F, of Fig. 2(a) differs in the stationary value by 14.8% from the G1–EN–S reference value and

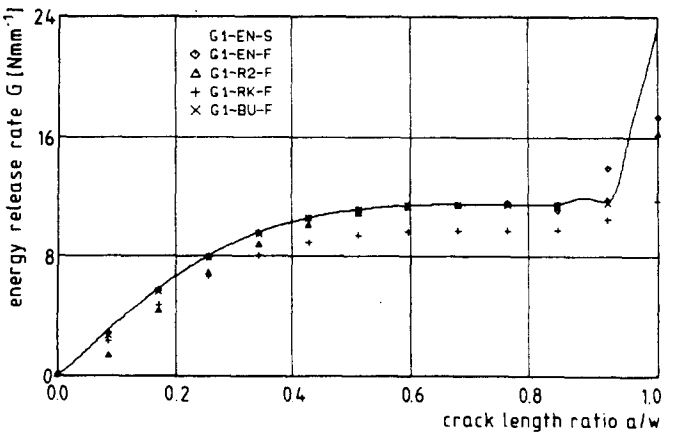

Fig. 7. Energy release rates calculated with the LSE-Formulae of 1st- and 2nd-Order and the fine LSE-net, F.

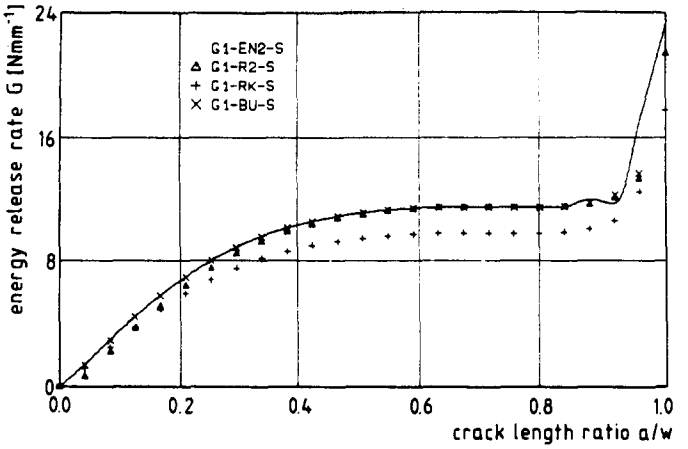

Fig. 8. Energy release rates calculated with the LSE-Formulae of 1st- and 2nd-Order and the superfine LSE-net, S.

the global accuracy measure [eqns (15)] delivers a deviation of $\Delta_{rel} = -18.8\%$. Figure 8 shows the corresponding results for the LSE-net, S, of Fig. 2(b). Using eqn (19) the stationary value of the G1–RK–S plot is still 14.8% too low compared with the reference value and $\Delta_{rel} = -16.4\%$ is a poor result with respect to the superfine net, S.

Because of these insufficient results eqn (19) has been reanalysed and on the basis of Irwin's crack closure integral and Rybicki and Kanninen's basic assumption the following LSE-Formula of 2nd-Order has been established by Buchholz

$$G_I(a) = \frac{1}{t} \lim_{\Delta a \to 0} \frac{1}{\Delta a} \frac{1}{2}(F_{y,i}(a)\Delta u_{y,i-2}(a) + F_{y,i+1}(a)\Delta u_{y,i-1}(a)). \tag{20}$$

Different from eqn (19), in eqn (20) two nodal point forces $F_{y,i}(a)$ and $F_{y,i+1}(a)$ at and in front of the crack tip (positions i and $i+1$ in Fig. 6(b)) are taken as approximations for the actually required forces at the positions $i-1$ and $i-2$. This approach is based on the knowledge that these forces are keeping the crack of length a closed along Δa in front of the actual crack tip, just at the corresponding nodal point positions $i-2$ and $i-1$ of the opened crack. Furthermore, in case of CS-Elements eqn (20) reduces to the CSE-Formula of 1st-Order [eqn (18)] given and used by Rybicki and Kanninen. Applying eqn (20) with admissible crack tip positions at corner nodes of the LS-Elements, respectively, this LSE-Formula of 2nd-Order delivers results with very good accuracy as can be seen in Figs. 7 and 8, respectively. Although eqn (20) works up a very limited amount of crack tip data for the calculation of the energy release rate $G_I(a)$ the G1–BU–F and –S plots in Figs. 7 and 8 nearly completely coincide with the G1–EN–S reference curve, calculated with the more laborious global energy method, EN. This results in a very good $\Delta_{rel} = -1.4\%$ for the G1–BU–F plot in Fig. 7 and an excellent $\Delta_{rel} = -0.4\%$ for the G1–BU–S plot in Fig. 8.

3.2. *J-Integral calculations*

In addition to the energy release rate calculations described above J-integral values for the straight central crack were calculated for a number of different crack lengths. The finite element program ADINA was used in combination with the post processor program JOTINT[15], which was developed at Brown, Boveri & Cie following the proposals by deLorenzi[7]. Hereby the method of virtual crack extension is applied as introduced by Hellen[4] and Parks[16]. In the paper of deLorenzi the following expression is derived for the calculation of the strain energy per unit thickness G^*, which is released by a virtual extension $\Delta\delta$ of the crack tip:

$$G^* = \int_V \left\{ \left(\sigma_{\alpha\beta} \frac{\partial u_\alpha}{\partial x_\delta} - W\delta_{\beta\delta} \right) \frac{\partial \Delta x_\delta}{\partial x_\beta} - f_\alpha \frac{\partial u_\alpha}{\partial x_\beta} \Delta x_\beta \right\} \mathrm{d}v, \tag{21}$$

where W, σ_{ij} and u_i are the strain energy and the components of the stress tensor and the displacements, respectively, in the volume of integration considered.

G^* and J are related by

$$G^* = J\,\Delta\delta. \tag{22}$$

Equation (21) gives the general three-dimensional relation for G^*. In a two-dimensional case as considered in this paper surface integrals have to be evaluated instead of line

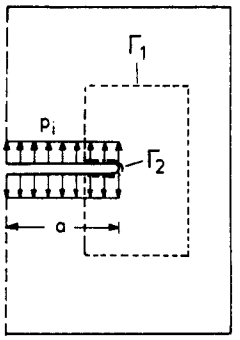

Fig. 9. J-Integral calculation of a crack with crack face loading.

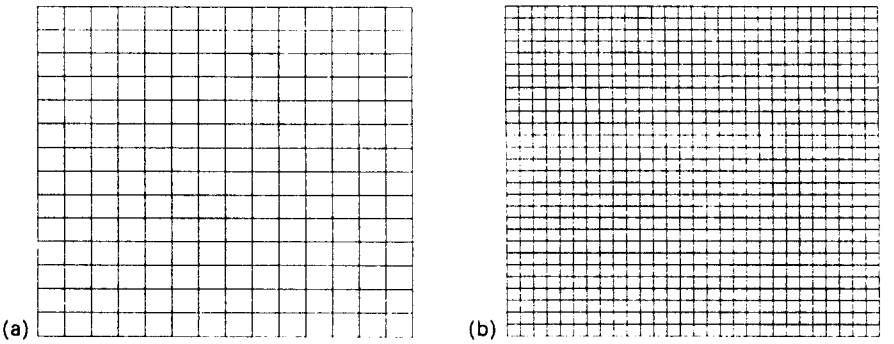

Fig. 10. Finite element nets of the specimen (one quarter) used for the ADINA calculations of $J(a)$. Quadrilateral 8-node "Linear Strain Elements" (LSE): (a) fine net, F, 196 elements, 645 nodal points; (b) superfine net, S, 784 elements, 2465 nodal points.

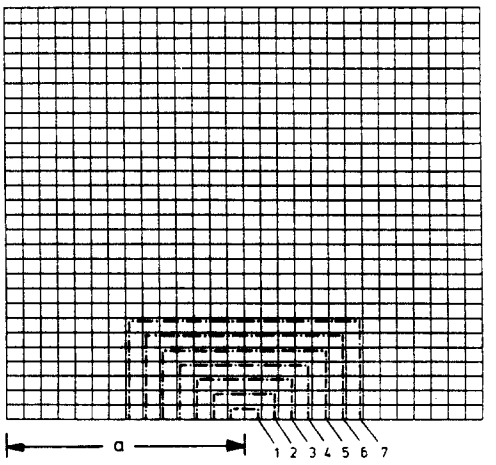

Fig. 11. Different integration paths for crack length ratio $a/w = 0.5$.

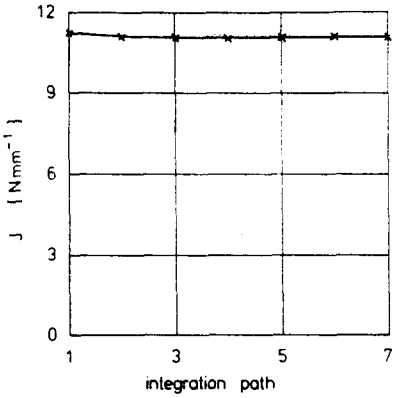

Fig. 12. Variation of J-integral values with different integration paths for the superfine net, S, and $a/w = 0.5$.

integrals, which are used in Rice's[5] original formulation. As the integration procedures included in ADINA can be used for the calculation of volume and surface integrals this is more convenient to do than to handle with line integrals.

DeLorenzi's formulation does not include thermal stresses and at the present time the program JOTINT also has no capability to handle thermal stress problems. To get meaningful results in our case, the superposition principle of linear elasticity was applied. The thermal stresses calculated for the uncracked strip were taken as pressure loading of the crack sufaces and the calculations were carried out for this problem. Furthermore, as the program JOTINT does not include crack face loadings, according to Fig. 9 the J-integral values were evaluated by addition of the two integration paths Γ_1 and Γ_2. The contribution Γ_1 was calculated by means of JOTINT, while the contribution of Γ_2 was evaluated by directly applying Rice's formula[5].

Figures 10(a) and (b) show the two finite element nets used for the calculations. In both cases 8-node linear strain elements were used. Net, F, referred to as fine net according to the nets for the ASKA-calculations, consists of 196 elements with 645 nodal points. Net, S, referred to as superfine net, is built up of 784 elements with 2465 nodal points.

Figure 11 shows the different integration paths used for the J-integral evaluation for the superfine net and $a/w = 0.5$. For the other crack lengths considered similar integration paths were used with the exception of $a/w = 0.0714$ and $a/w = 0.9286$, respectively, where only path 1 (for the fine net) and paths 1 and 2 (for the superfine net) could be evaluated.

Figure 12 shows J-integral values for the different integration paths for $a/w = 0.5$ and the superfine structure. As can be seen the path independence of the J-integral is fulfilled rather well. A summary of the results of the J-integral calculations is given in Table 1.

In Fig. 13 the J-integral values are compared with energy release rate results by Buchholz and Meiners[13] calculated with the global energy method, EN, derived from energy calculations. The coincidence of the results can be considered as very good, except for $a/w = 0.0714$ and $a/w = 0.9286$. The deviations in these cases may be explained by the fact that for these two crack lengths only integration path 1 or 1 and 2, respectively, could be evaluated.

Table 1. Results of the J-integral calculations

a/w	Fine net (J/Nmm^{-1})	Superfine net (J/Nmm^{-1})
0.0714	2.74	2.62
0.2857	8.65	8.69
0.5000	11.04	11.04
0.6429	11.40	11.39
0.9286	13.04	12.79

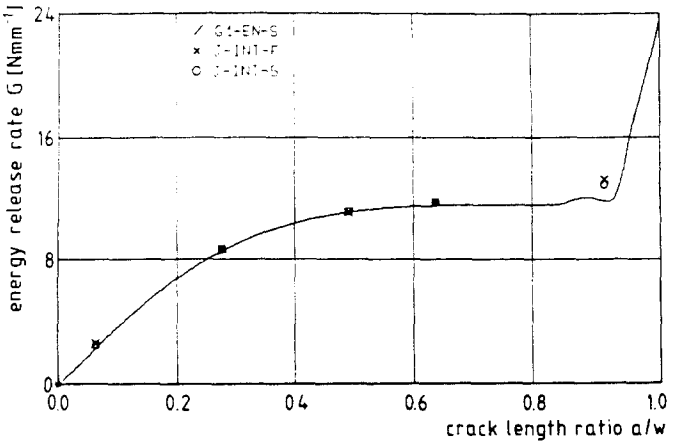

Fig. 13. Comparison of J-integral values $J(a)$, calculated with ADINA and JOTINT and energy release rates $G(a)$, calculated with the global energy method, EN and ASKA.

4. CONCLUSIONS

The numerical investigations of this paper have shown that the energy release rate $G(a)$ can be calculated with very good accuracy by different global or local energy methods, in combination with standard finite elements of higher order (LSE) and without requiring net refinements adjacent to the crack tip. The quality of the numerical results has been indicated by the aid of an analytically based accuracy measure established for this specially supported and loaded specimen. Besides the simplicity of the procedure the original and the improved modified crack closure integral method has the advantage to deliver simultaneously the separated $G_i(a)$-values, $i = \mathrm{I}, \mathrm{II}$ for plane mixed mode problems[8, 17] and furthermore, that the method can be generalized successfully for the analysis of 3D-fracture problems of composite materials (thermally loaded curved interface cracks) generating simultaneously all three fracture modes[18].

REFERENCES

1. S. K. Chan, I. S. Tuba and W. K. Wilson, On the finite element method in linear fracture mechanics. *Engng Frac. Mech.* **2**, 1–17 (1970).
2. D. J. Hayes, A practical application of Bückner's formulation for determining stress intensity factors for cracked bodies. *Int. J. Fract. Mech.* **8**, 157 (1972).
3. G. P. Anderson, V. L. Ruggles and G. S. Stibor, Use of finite element computer programs in fracture mechanics. *Int. J. Fract. Mech.* **7**, 63–76 (1971).
4. T. K. Hellen, On the method of virtual crack extensions. *Int. J. Num. Meth. Engng* **9**, 187–207 (1975).
5. J. R. Rice, A path independent integral and the approximate analysis of strain concentration by notches and cracks. *J. Appl. Mech.* **35**, 379–386 (1968).
6. D. M. Parks, A stiffness derivative finite element technique for determination of crack tip stress intensity factors. *Int. J. Fracture* **10**, 487–502 (1974).
7. H. G. deLorenzi, On the energy release rate and the J-integral for 3D-crack configurations. *Int. J. Fracture* **19**, 183–193 (1982).
8. E. F. Rybicki and M. F. Kanninen, A finite element calculation of stress intensity factors by a modified crack closure integral. *Engng Frac. Mech.* **9**, 931–938 (1977).
9. S. Timoshenko and J. N. Goodier, *Theory of Elasticity*. McGraw-Hill, New York (1970).
10. O. C. Zienkiewicz, *The Finite Element Method in Structural and Continuum Mechanics*. McGraw-Hill, London (1967).
11. F.-G. Buchholz, Einflüsse von Elementtyp und Netztopologie auf die FE-Berechnung eines modifizierten Rißschließungsintegrals. *Proc. XIth Int. FEM-Congr.*, Baden-Baden, F.R.G. (Edited by IKOSS GmbH), pp. 77–101. Stuttgart (1982).
12. F.-G. Buchholz and K. Herrmann, A note on generalized applications of the modified crack closure integral. *Proc. 3rd Int. Conf. on Num. Meth. in Fract. Mech.*, Swansea, U.K., pp. 149–163. Pineridge Press, Swansea (1984).
13. F.-G. Buchholz and B. Meiners, On the accuracy of the modified crack closure integral method in combination with higher order finite elements. *Proc. Int. Conf. on Accuracy Estimates and Adaptive Refinements in Finite Element Computations*, Lisbon (Edited by CMEST), pp. 131–140. University of Lisbon (1984).
14. G. R. Irwin, Fracture. *Handbuch der Physik* 6, pp. 551–590. Springer, Berlin (1958).

15. U. Strathmeier and H. Grebner, JOTINT—Ein Programm zur Berechnung des J-Integrals. *Pres. at GAAM Annual Meeting* 1984. *ZAMM* **65**, T168–170 (1985).
16. D. M. Parks, The virtual crack extension method for non-linear material behavior. *Comp. Meth. Appl. Mech. Engng* **12**, 353–364 (1977).
17. F.-G. Buchholz, Improved formulae for the FE-calculation of the strain energy release rate by the modified crack closure integral method. *Proc. 4th World Congr. and Exhib. on Finite Element Methods*, Interlaken (Edited by Robinson and Associates), pp. 650–659. Dorset, U.K. (1984).
18. F.-G. Buchholz, B. Meiners and K. Herrmann, Numerische Untersuchungen zur Methode des modifizierten Rißschließungsintegrals. *DVM-Bericht*, **17**. Sitzung Arbeitskreis Bruchvorgänge, pp. 427–438. Basel (1985).